



Discriminant analysis of pyrrolizidine alkaloid contamination in bee pollen based on near-infrared data from lab-stationary and portable spectrometers

Luciana De Jesus Inacio¹ · Ilaria Lanza² · Roberta Merlanti¹ · Barbara Contiero² · Lorena Lucatello¹ · Lorenzo Serva² · Vittoria Bisutti² · Massimo Mirisola² · Sandro Tenti² · Severino Segato² · Francesca Capolongo¹

Received: 23 June 2020 / Revised: 6 August 2020 / Accepted: 10 August 2020 / Published online: 29 August 2020
© The Author(s) 2020

Abstract

Bee pollen may be contaminated with pyrrolizidine alkaloids (PAs) and their *N*-oxides (PANOs), which are mainly detected by liquid chromatography coupled to tandem mass spectrometry (LC–MS/MS), even though the use of fast near-infrared (NIR) spectroscopy is an ongoing alternative. Therefore, the main challenge of this study was to assess the feasibility of both a lab-stationary (Foss) and a portable (Polispec) NIR spectrometer in 60 dehydrated bee pollen samples. After an ANOVA-feature selection of the most informative NIR spectral data, canonical discriminant analysis (CDA) was performed to distinguish three quantitative PA/PANO classes ($\mu\text{g}/\text{kg}$): < LOQ (0.4), low; 0.4–400, moderate; > 400, high. According to the LC–MS/MS analysis, 77% of the samples were contaminated with PAs/PANOs and the sum content of the 17 target analytes was higher than 400 $\mu\text{g}/\text{kg}$ in 28% of the samples. CDA was carried out on a pool of 18 (Foss) and 22 (Polispec) selected spectral variables and allowed accurate classification of samples from the low class as confirmed by the high values of Matthews correlation coefficient (≥ 0.91) for both NIR spectrometers. Leave-one-out cross-validation highlighted precise recognition of samples characterised by a high PA/PANO content with a low misclassification rate (0.02) as false negatives. The most informative wavelengths were within the < 1000, 1000–1660 and > 2400 nm regions for Foss and > 1500 nm for Polispec that could be associated with cyclic amines, and epoxide chemical structures of PAs/PANOs. In sum, both lab-stationary and portable NIR systems are reliable and fast techniques for detecting PA/PANO contamination in bee pollen.

Keywords Pyrrolizidine alkaloids · Bee pollen · LC–MS/MS · NIR spectroscopy · Canonical discriminant analysis

Introduction

Bee pollen is a mixture of flower pollen, nectar and bee saliva. This beehive product is rich in essential nutrients and biologically active substances, such as phenolic compounds that can exhibit antioxidant, anti-inflammatory and anti-microbial activity. Thus, the consumption of bee pollen as a food supplement and a health product has increased in recent years [1]. However, depending on the geographical and botanical origin, bee pollen might be potential hazard

for human intake due to the presence of natural toxins like pyrrolizidine alkaloids (PAs) and their *N*-oxides (PANOs) [2].

PAs/PANOs are secondary metabolites produced by plants as a chemical defence against herbivorous insects. They are predominant in all genera of the Boraginaceae family, in the Senecioneae and Eupatorieae tribes (Asteraceae), but they are also present in the genus *Crotalaria* (Fabaceae) [3]. PAs/PANOs have been reported to cause toxicity in many animal species, including humans. Experimental data obtained from in vitro and in vivo studies suggest that chronic exposure to PAs/PANOs may lead to hepatotoxicity, genotoxicity, carcinogenicity and pulmonary lesions [4, 5]. However, the toxicity of PAs/PANOs is dependent on their chemical structure [6]. Only those compounds that contain a double bond at the 1,2-position of the necine base can be transformed into highly reactive pyrroles in the liver. Furthermore, PAs/PANOs can be classified according to their

✉ Roberta Merlanti
roberta.merlanti@unipd.it

¹ Department of Comparative Biomedicine and Food Science, University of Padova, 35020 Legnaro, PD, Italy

² Department of Animal Medicine, Production and Health, University of Padova, 35020 Legnaro, PD, Italy

esterification level as cyclic diesters, open-chain diesters and monoesters, which are in decreasing order of toxicity [4–6]. Based on botanical origin and chemical structure, PAs/PANOs can be classified into different groups, such as lycopsamine, senecionine and heliotrine types [3]. The lycopsamine-type PAs/PANOs consist of monoesters (e.g., lycopsamine and its *N*-oxide, indicine *N*-oxide, intermedine) and open-chain diesters (e.g., echimidine and its *N*-oxide) produced by plants from the Boraginaceae and tribe Eupatorieae. The senecionine-type compounds are cyclic diesters (e.g., jacobine, retrorsine, senecionine, seneciphylline and their *N*-oxides, and senkirkinine), particularly found in plants from the tribe Senecioneae, while the heliotrine-type PAs/PANOs are monoesters (e.g., heliotrine and its *N*-oxide) that occur in the genus *Heliotropium* (Boraginaceae) [3].

Although PAs/PANOs can cause toxic effects, it has not yet been possible to establish a limit in food and feed due to analytical uncertainties [7]. In addition, there is a lack of toxicological data relating to the PAs/PANOs found most frequently in food [8]. Some authorities, such as the European Food Safety Authority (EFSA), have performed independent risk assessments by applying the margin of exposure (MOE) approach, based on the benchmark dose lower confidence limit for a 10% excess cancer risk (BMDL₁₀) derived from animal studies. In this approach, an MOE value of at least 10,000 is of low concern for carcinogenic effects [3]. In 2011, the EFSA proposed an orientation value of 0.007 µg/kg body weight (b.w) for the sum content of PAs/PANOs, based on a BMDL₁₀ of 70 µg/kg b.w/day of lasiocarpine in male rats, and an MOE value of 10,000 [3, 9, 10]. In 2017, the EFSA updated its risk characterisation using the MOE approach and a new BMDL₁₀ of 237 µg/kg b.w, derived from the incidence of liver haemangiosarcoma in female rats exposed to riddelliine [8]. Thus, an orientation value of 0.024 µg/kg b.w/day for the sum of PAs/PANOs could be considered of low concern for public health [11]. Regarding non-carcinogenic risks, with PA/PANO concentrations lower than 0.1 µg/kg b.w/day, these kinds of effect are not expected to occur [10]. This orientation value was obtained from a No Observed Adverse Effect Level (NOAEL) for riddelliine in rats of 10 µg/kg b.w/day, divided by an uncertainty factor of 100 [10]. Based on data published by EFSA [12], possible limits for PAs/PANOs in those foods that most contribute to human exposure through the diet are currently being discussed at European Union level [13]. Maximum PA/PANO levels of 400 and 500 µg/kg have been proposed for pollen products [14, 15]. Nevertheless, given that intake of even low PA/PANO amounts could increase the risk to health, especially if consumed frequently, the recommendation is still that the intake of these natural toxins should be minimised to the lowest level possible [16]. For this reason, the EFSA recommends the development of more sensitive methods to detect PAs/PANOs in food [8].

The main methods for analysis of PAs/PANOs are based on liquid chromatography coupled to tandem mass spectrometry (LC–MS/MS), which is highly sensitive, specific and reliable [17–19] but also time-consuming and expensive. Therefore, there is a need to develop fast, non-destructive, cost-effective and multi-modality analytical methods that support at-line control of natural toxins throughout the supply chain. Near-infrared (NIR) spectroscopy is a powerful technology that has been already proposed in food-contaminant monitoring related to human health concern [20]. Hence, there is an ongoing increase in the application of NIR to detect mycotoxins [21, 22], allergens [23] and gluten [24] in food products, even at low levels (µg/kg). However, to the best of our knowledge, NIR spectroscopy applications for the detection of PAs/PANOs in bee pollen or analogous food supplements have not yet been performed. So far, only Carvalho et al. have reported the potential of NIR to predict the PA/PANO content in fresh and dried leaves of three *Senecio* species [25]. Furthermore, there is a lack of literature on the feasibility of applying miniaturised and portable spectroscopic devices, which could further raise the rapidity of measurement as well as avoiding the transportation of samples to the laboratory [26, 27].

In this context, this study first aimed to evaluate the distribution of PAs in bee pollen through univariate analysis across a classification criterion based on 400 µg/kg that could be considered a potential threshold of compliance in line with the future policy of food safety authorities. Regardless of the compliance limit, there is a need for rapid detection of these natural toxins in food, a challenge that could be reliably met by NIR spectroscopy technique. Thus, the main goal of this trial was to assess the feasibility of two NIR systems by means of a statistical modelling approach based on targeted canonical discriminant analysis (CDA). To achieve these aims, 60 bee pollen samples were analysed by a validated LC–MS/MS method, suitable for detecting and quantifying 17 PAs/PANOs suggested by EFSA to be monitored in food.

Materials and methods

Sampling and experimental design

Sixty dehydrated bee pollen samples were purchased from stores and online shops from different countries (39 from Italy, 17 from EU countries, 4 from non-EU countries). Based on standard guidelines and literature data, the samples were supposed to have a moisture level lower than 6% [28, 29]; therefore, they were kept in a dark, cool and dry place until analysis by LC–MS/MS and NIR spectroscopy. Approximately 50 g of each bee pollen sample was ground and homogenised by a GRINDOMIX GM 200 mill (Retsch,

Italia, Torre Boldone, Italy) at 6000 rpm for 15 s. The NIR spectral data collection and LC–MS/MS analysis were carried out on ground bee pollen.

LC–MS/MS analysis

Standards, solvents and reagents

Analytical standards were obtained from different suppliers as follows: echimidine (purity 97%), echimidine *N*-oxide (purity 97%), heliotrine (purity 91%), heliotrine *N*-oxide (purity 91%), lycopsamine (purity 80%) and lycopsamine *N*-oxide (purity 80%) from PhytoLab GmbH & Co. KG (Vestenbergsgreuth, Germany); senecionine (purity 99%), senecionine *N*-oxide (purity 99%), seneciphylline (purity 94%) and seneciphylline *N*-oxide (purity 94%) from Carl Roth & Co. KG (Karlsruhe, Germany); indicine-*N*-oxide (purity 99%), intermedine (purity 99%), jacobine (purity 98%), jacobine *N*-oxide (purity 98%), retrorsine (purity 90%), retrorsine *N*-oxide (purity 96.0%) and senkirkine (purity 98%) from Phytoplan (Heidelberg, Germany); caffeine (purity 98%), used as an internal standard, was from Sigma-Aldrich (Steinheim, Germany).

Methanol (LC–MS grade) and sulphuric acid (98% purity, analytical grade) were from Carlo Erba reagents (Milan, Italy). Ammonia (28% purity, analytical grade) was from VWR Chemicals. Formic acid (98% purity, LC–MS grade) was from Sigma-Aldrich. Ultra-pure water was obtained from a water purification system (Purelab Classic, ELGA Lab Water, High Wycombe, UK).

Sample preparation and LC–MS/MS analysis

Sample preparation, PA/PANO extraction from bee pollen samples and LC–MS/MS analysis were performed as described by De Jesus Inacio et al. [30]. The validated LC–MS/MS method used in this work is suitable for detecting and quantifying 17 PAs/PANOs in bee pollen. Detailed information on the analytical parameters (specificity, linearity, apparent recovery, precision, absolute recovery and matrix effect) evaluated in the LC–MS/MS method validation for target PAs/PANOs were reported in De Jesus Inacio et al. [30].

Briefly, the PAs/PANOs were extracted from 2.5 g of ground bee pollen samples using 15 mL of 0.05 M sulphuric acid solution. After 10 min of shaking, 10 mL of *n*-hexane was added and the samples were shaken for another 10 min and centrifuged at 3000g for 10 min. The organic phase was discarded and the aqueous extracts were then applied onto strong cation polymeric solid phase cartridges (Bond Elut Plexa PCX, 200 mg/6 mL, Agilent), previously conditioned with 6 mL methanol and 6 mL 0.1% formic acid in water. After loading, the cartridges were washed with

3 mL methanol and then eluted with 6 mL of 5% ammonia in methanol. The eluates were dried under an air stream at 50 °C, re-suspended with 1 mL of caffeine (internal standard, 500 ng/mL) in 0.1% formic acid in methanol and 0.5% formic acid in water (20:80, v/v) and filtered with a syringe filter consisting of a 0.22- μ m regenerated cellulose (RC) membrane [31]. The PA/PANO extracts were analysed using a high-performance liquid chromatography system consisting of an Accela 600 HPLC pump equipped with a CTC automatic injector (Thermo Fischer Scientific, San Jose, CA, USA) and coupled to an LTQ XL ion trap mass spectrometer (Thermo Fischer Scientific, San Jose, CA, USA) with a heated electrospray ionisation (HESI-II) probe. Five microliters of extract samples was loaded onto the analytical column (Hypersil GOLD 100 \times 2.1 mm, 1.9 μ m, Thermo Fisher Scientific, San Jose, CA, USA), and the PA/PANO separation was performed in a gradient of solvent A (water with 0.1% formic acid) and B (methanol with 0.1% formic acid) at a flow rate of 200 μ L/min as follows: isocratic condition from 0 to 4 min (90% A and 10% B); from 10 to 15% (B) in 0.5 min; 15% (B) from 4.5 to 9 min; from 15 to 40% (B) in 5 min; from 40 to 80% (B) in 1 min; 80% (B) for 1.5 min; from 80 to 10% (B) in 0.5 min; from 17 to 20 min 10% (B) to re-equilibrate the column.

The 17 PAs/PANOs were detected by the MS with the ESI source operating in positive-ion mode. The optimised operational LC–ESI(+)-MS/MS and detection conditions used for all the PAs/PANOs were as follows: sheath gas flow, 35 arbitrary units; auxiliary gas flow, six arbitrary units; ion spray voltage, 3.5 kV; capillary temperature, 350 °C; capillary voltage, 11 V; and tube lens, 60 V. The MS/MS conditions (collision energy, precursor and product ions) and the retention times obtained for each analyte were reported in Inacio et al. [30].

The limit of quantification (LOQ) of each PA/PANO was set at 0.4 μ g/kg which is the lowest calibrator concentration on the calibration curve that could be quantified with a precision within 20%, and trueness between 80 and 120% as reported by the European Commission Decision 2002/657/EC [30].

The concentration of individual PAs/PANOs was calculated based on calibration curves prepared with a pool of blank bee pollen spiked with the 17 PAs/PANOs prior to the extraction to obtain the final concentration in the range 0.4–100 μ g/kg.

NIR analysis

All bee pollen samples were analysed in triplicate using both a FOSS DS-2500 scanning monochromator (FOSS NIRSystem, Hillerød, Denmark) and portable NIR apparatus (PoliSPEC^{NIR}, ITPhotonics, Breganze, Italy). In the case of the lab-stationary system (referred to as Foss), scans

were recorded in reflectance mode (850–2500 nm at 0.5-nm intervals) using a slurry cup with a quartz window (12.6 cm² area) in 30 g aliquots. With regard to the portable system (referred to as Polisppec), scans were also performed in reflectance mode (902–1670 nm at 2-nm intervals) using a quartz cylinder (9.1 cm² area) in 5 g aliquots. Spectral data were recorded as absorbance (*A*) calculated as $\log(1/R)$, where *R* represents reflectance, using WinISI4 software V4.10.0.15326 (FOSS Analytical A/S, Hillerød, Denmark) for Foss and using poliDATA (ITPhotonics, Breganze, Italy) for Polisppec. For both systems, to carry out the statistical analysis, spectra were exported to an Excel (Microsoft Office®, USA) spreadsheet and averaged before further chemometric modelling.

Data and statistical analysis

The 60 bee pollen samples analysed were grouped into three quantitative (µg/kg) classes according to the sum of the 17 PAs/PANOs: < LOQ (0.4), low; 0.4–400, moderate; and > 400, high. As the PA/PANO data were not normally distributed, a Kruskal–Wallis test was carried out to analyse the effect of the distribution of these alkaloids within the three quantitative classes (XLSTAT, Addinsoft, release 2019, NY, USA). To evaluate the classifying effect, a multiple pairwise comparison was conducted using the Steel–Dwass–Critchlow–Fligner procedure (based on the averaged rank).

The variable importance in projection (VIP) indices were calculated using the relevance of predictors according to the threshold criterion of ‘greater than one’ of the PLS-DA algorithm [32], by means of MATLAB R2017a software V9.2.0.538062 (The MathWorks Inc., Natick, MA, USA) and PLS Toolbox (PLS Toolbox V5.8.2.1, Eigenvector Research Inc., Manson, WA, USA).

To discriminate the PA/PANO classes, a supervised CDA was also adopted for each NIR spectrometer (SAS 9.4 software, SAS Institute Inc., Cary, NC, USA). The first step was processing of the Foss dataset to reduce the number of wavelengths. For this purpose, the absorbance (*A*) was averaged every 8-nm interval, and the mean value was assigned to the intermediate wavelength (i.e., λ_{854} is equal to the average of *A* from 850 to 858 nm, λ_{2494} is equal to the average of *A* from 2492 to 2500 nm). The second step was a stepwise feature selection based on analysis of variance (ANOVA) to select those significant ($p < 0.05$) spectral variables related to the PA/PANO classes. CDA was performed on the selected spectral variables (PROC CANDISC of SAS), to explain the total variance of the model in two main canonical functions (CAN 1 and CAN 2). The degree of dissimilarity among the three quantitative PA/PANO classes was measured by squared Mahalanobis distances (D^2 -Mahalanobis).

The reliability of the CDA model was assessed by a confusion matrix obtained by means of a cross-validation based on the leave-one-out criterion (PROC DISCRIM of SAS). As suggested by Bisutti et al. [33], the reliability of the related confusion matrix was evaluated by a set of statistical metrics: accuracy, precision, sensitivity, specificity and Matthews correlation coefficient (MCC).

Results and discussion

LC–MS/MS analysis and distribution of PAs/PANOs in bee pollen

LC–MS/MS analysis of the 60 dehydrated bee pollen samples was performed according to a validated method published in a previous study [30].

PAs/PANOs were found in 46 (77%) of the 60 bee pollen samples and the sum amounts of the detected compounds were noticeably distinct (from 2 to 3356 µg/kg); a detailed framework of the descriptive statistics is reported in Table 1. In 17 (37%) of the contaminated samples, the sum of PA/PANO concentration was over the value of 400 µg/kg, which has been considered as threshold for further analyses performed in this study. Lycopsamine-type PAs/PANOs were found in the majority (85%) of the contaminated bee pollen samples, followed by senecionine-type (48%) and heliotrine-type PAs/PANOs (11%) that were rarely found. Figure 1 summarises the descriptive statistics of the main individual and total PAs/PANOs within the three quantitative classes through univariate non-parametric analysis. There was a predominance of echimidine, echimidine *N*-oxide and lycopsamine. The most noticeable feature is that there is high variability in the distribution of the PA/PANO concentration within the high class, while it is negligible for the moderate class. This is especially observed for lycopsamine (Fig. 1a), senecionine and seneciphylline *N*-oxides (Fig. 1b), while for echimidine and echimidine *N*-oxide (Fig. 1a), the range of variability is much lower and the distribution of samples is quite close to the median value.

The results of this trial are in agreement with those published by Mulder et al. [17] and Picron et al. [18] who also reported a similar pattern for PAs/PANOs in bee pollen, with echimidine and its *N*-oxide as the main contributors to the sum content of these natural toxins. Even though the LC–MS/MS methods used by these authors cover a higher number of analytes (28–30), most of the additional compounds, including lasiocarpine and its *N*-oxide, have not been detected or they were found at trace levels and therefore, such compounds do not contribute remarkably to sum of PA/PANO concentration. Furthermore, the PA/PANO composition identified in the bee pollen samples, is also in agreement with that

Table 1 Descriptive statistics of the 17 pyrrolizidine alkaloids (PAs) and PA *N*-oxides (PANOs) and ΣPAs/PANOs (μg/kg) monitored in bee pollen

Analytes	Range	Mean (± sd)	Percentiles			nd (n)
			10th	50th	90th	
Echimidine	0–2128	124 (332)	0	0	316	33
Echimidine <i>N</i> -oxide	0–2078	96 (310)	0	0	254	32
Jacobine	–	–	–	–	–	60
Jacobine <i>N</i> -oxide	–	–	–	–	–	60
Indicine <i>N</i> -oxide	0–318	20 (58)	0	0	47	32
Intermidine	0–246	10 (34)	0	0	34	32
Lycopsamine	0–418	30 (77)	0	1	115	27
Lycopsamine <i>N</i> -oxide	0–368	23 (61)	0	0	92	30
Retrorsine	0–109	2 (14)	0	0	3	52
Retrorsine <i>N</i> -oxide	0–953	17 (123)	0	0	0	57
Senkirkine	–	–	–	–	–	60
Senecionine	0–64	6 (16)	0	0	22	47
Senecionine <i>N</i> -oxide	0–297	19 (59)	0	0	74	44
Seneciphylline	0–173	8 (27)	0	0	24	45
Seneciphylline <i>N</i> -oxide	0–679	24 (104)	0	0	30	49
Heliotrine	0–2	0 (0)	0	0	0	57
Heliotrine <i>N</i> -oxide	0–11	0 (2)	0	0	0	55
ΣPAs/PANOs	0–3356	382 (736)	0	32	1081	14

nd number (*n*) of samples where the analytes were not detected; sd standard deviation

reported for honeys from Europe [18, 34]. In addition, the data from this work underline the high variability of the presence of PAs/PANOs in bee pollen, as observed for lycopsamine (Fig. 1a) and senecionine *N*-oxide (Fig. 1b). This phenomenon is probably due to the fact that bees collect pollen from both plants that do not synthesise these toxins and PA-producing plants [18]. Indeed, both the PA/PANO concentration and composition depend on the botanical taxon, geographical origin [35] and developmental stage of the plants. Moreover, synthesis of PAs/PANOs by plants is influenced by many other agronomic and environmental factors such as soil fertility, water availability and climate conditions [36–38]. Since most bee pollen samples analysed were from Italy and other European countries, possible sources of the lycopsamine-type PAs/PANOs could be plants from the genus *Echium* (e.g., *E. vulgare*), which is known to produce high levels of echimidine and its *N*-oxide, and *Borago officinalis* and *Eupatorium cannabinum* that synthesise lycopsamine, lycopsamine *N*-oxide and their isomers. *Echium* and *Borago* species are abundant in the Mediterranean region [39, 40], while *Eupatorium cannabinum* is diffuse in Europe [40]. Regarding senecionine-type PAs/PANOs, their origin could be *Senecio* species, which are widely distributed in Europe and grow everywhere [25, 39]. Although these plants are abundant, if other more attractive pollen sources are available, bees may prefer them

[40], and this could also explain the high variability of the PA/PANO concentration and frequency in bee pollen.

NIR spectral data and discriminant analysis of PAs/PANOs

The development of a rapid spectroscopic method in the detection of PAs/PANOs in food supplements was the main challenge of this trial. For food safety purposes, this challenge was to verify if NIR combined with a statistical modelling approach could be a feasible technique to discriminate bee pollen samples grouped into three classes according to their PA/PANO content.

NIR spectra

The NIR spectral data were recorded for ground bee pollen because the grinding process tends to improve the discriminative performance. As reported by Pasikitan et al. [41], NIR analysis is sensitive to the particle size and homogeneity of the matrix, both of which can affect the spectra and, consequently, the predictive performance. Thus, to guarantee a satisfactory precision in discriminative analyses, a grinding step is useful to obtain a more homogeneous matrix and reduce the light scattering effects that result in spectral noise. In the previous study of De Jesus

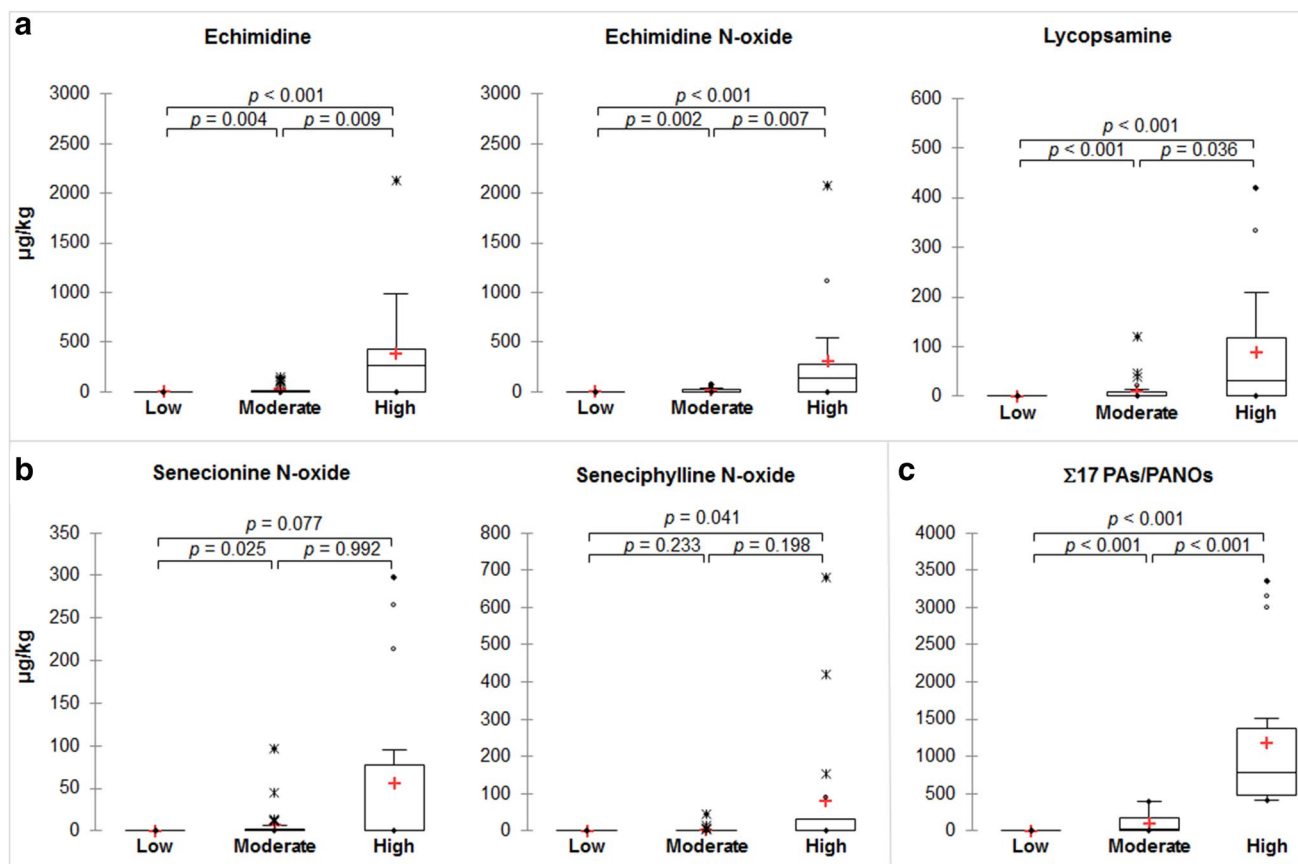


Fig. 1 Box-whisker plots of lycopamine-type (a) and senecionine-type compounds (b) and total PAs/PANOs (c) according to the three quantitative (µg/kg) PA/PANO classes (<LOQ (0.4), low; 0.4–400, moderate; and >400, high). The box plots represent the following descriptive statistics: median (bar in box), mean (+, red cross), 25–75% quartile (bottom and top end of the box), minimum and

maximum values (whiskers) except for outliers (°circles, distance to box 1.5–3.0 times interquartile range) and extreme values (*asterisks, distance to box >3 times interquartile range). The significance (*p* values on the top) of the multiple comparisons among the three PA/PANO classes was determined by Kruskal–Wallis non-parametric test

Inacio et al. [30], which tested the capability of a visible spectrophotometer to predict the presence of PAs/PANOs in bee pollen, the highest correlation between PA/PANO amount and the spatial colour coordinate named lightness was observed in ground samples.

Figure 2 evidences the averaged NIR spectra of the three quantitative PA/PANO classes. For both NIR systems, in the first part of the spectrum region (< 1450 nm), there was overlapping of the absorbance (*A*) among the three classes, while the absorbance of the low class was noticeably separated from the other two classes at higher wavelengths (> 1500 nm). In the study of González-Martín et al. [42], which applied NIR spectroscopy to assess bee pollen quality parameters, the spectra seemed to be comparable to those of the Foss system, with a meaningful absorbance peak around 1950 nm and a subsequent increasing trend up to 2500 nm. Costa et al. [43] reported a similar absorbance profile, although they analysed samples with a Fourier transform (FT)-NIR system. With regard

to the portable system, it was not possible to confirm the absorbance pattern with data from the literature. The main outcomes of this alternative NIR instrument are an increasing absorbance from 1450 nm and *A* values about half of the Foss ones.

The VIP scores chart obtained for each NIR spectrometer is shown in Fig. 3. The VIP pathway was characterised by intense peaks (VIP scores > 1) in the < 1000, 1000–1660 and > 2400 nm regions for Foss and only > 1500 nm for Polispec. The explicative VIP predictors showed an overlap between low and moderate classes throughout almost all the spectral range of the Foss system, meaning that the informative bands correlated with the smallest or medium PA/PANO content involved similar dominant wavelength regions. In contrast, the Foss-VIP pattern of the high class was almost distinguished from the other ones, and its explicative predictors (VIP scores > 1) belonged to the 900–1350-nm region.

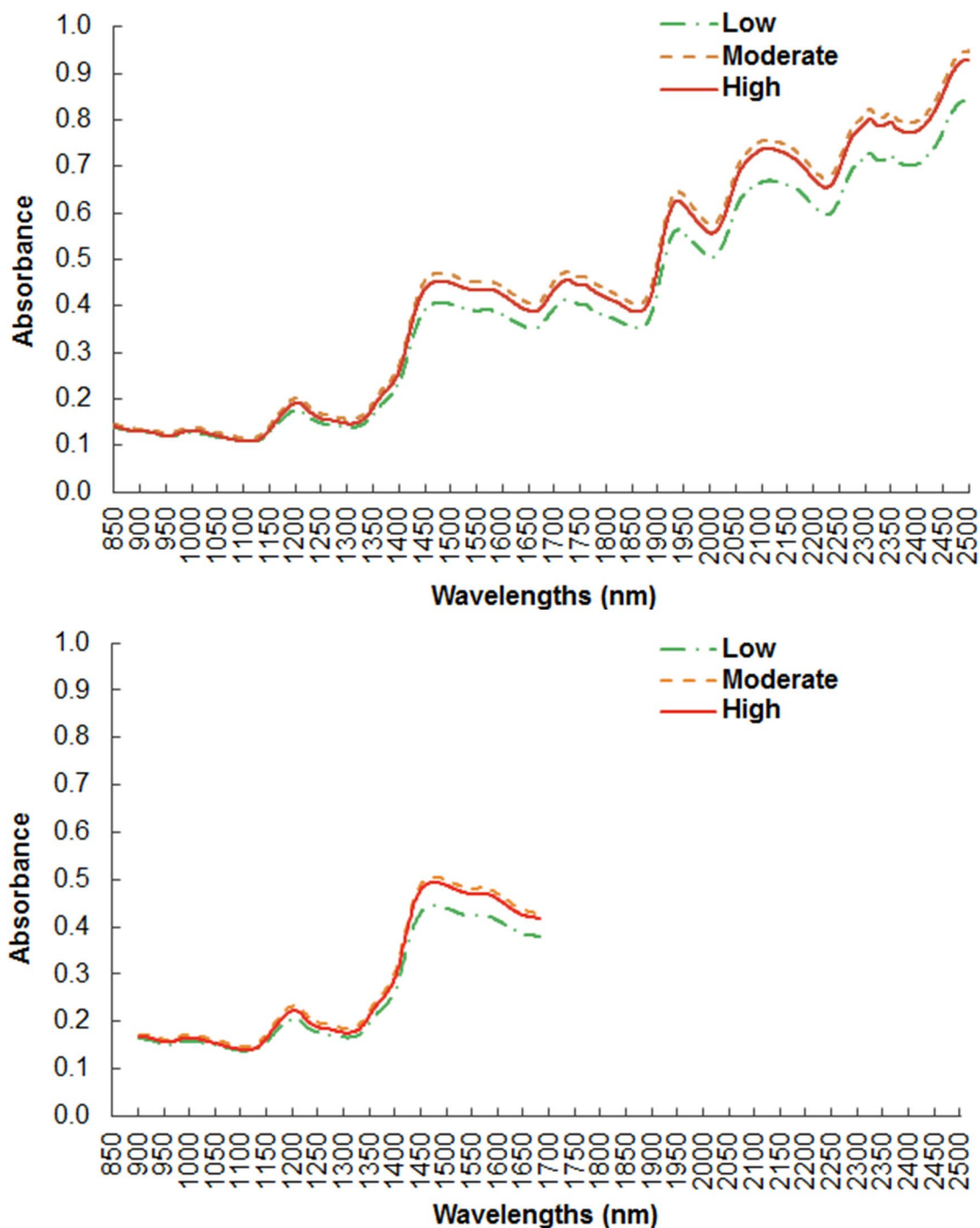


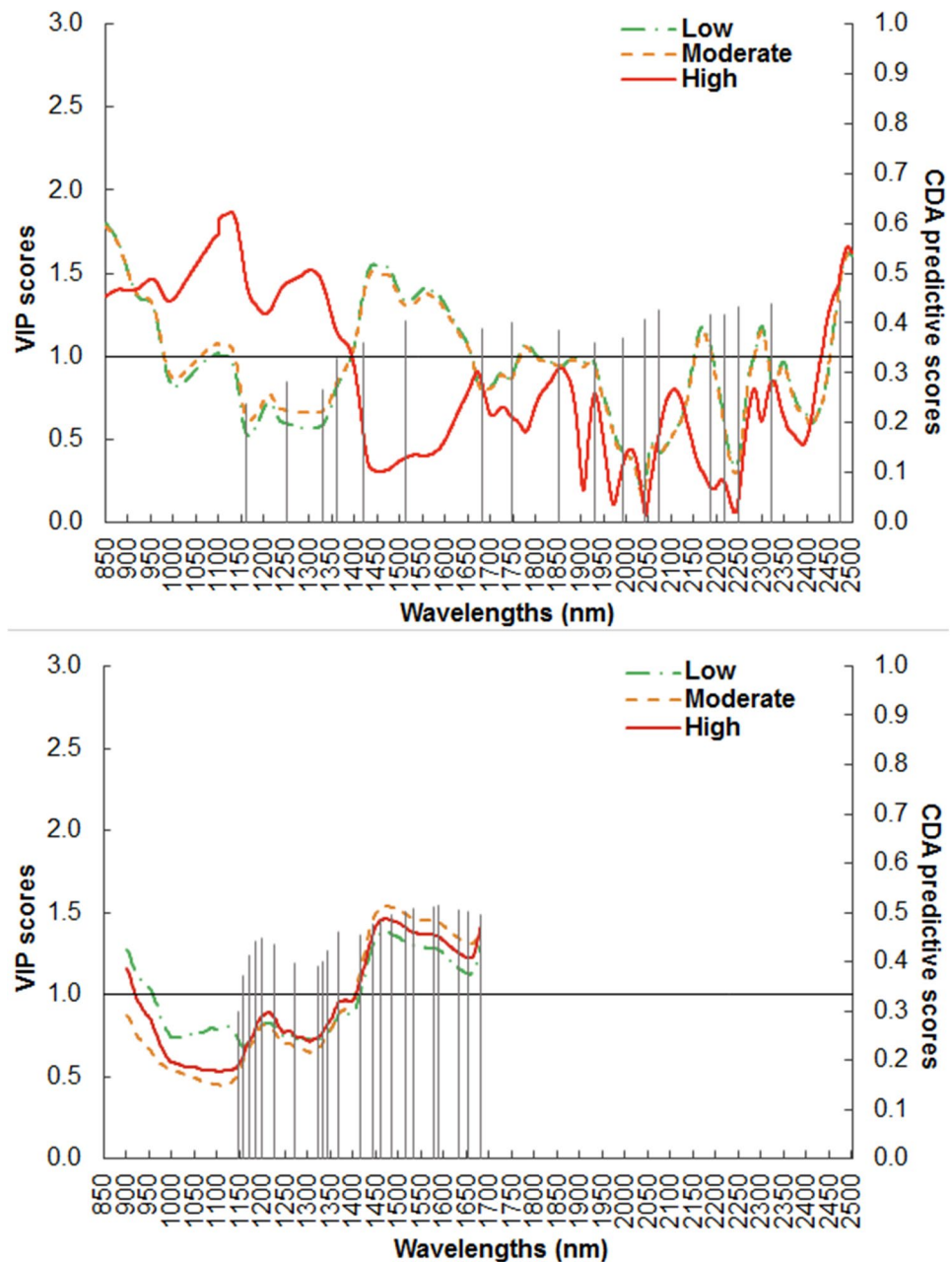
Fig. 2 Absorbance spectra for the three quantitative classes of pyrrolizidine alkaloids (PAs) and their *N*-oxides (PANOs) in bee pollen, based on lab-stationary (Foss, upper panel) and portable (Polispec,

lower panel) near-infrared (NIR) systems. Quantitative ($\mu\text{g}/\text{kg}$) PA/PANO classes: <LOQ (0.4), low; 0.4–400, moderate; > 400, high

However, in the last part of the spectrum (> 2400 nm) there was a similar trend among the three classes. In the case of the portable NIR system, the VIP pathway was characterised by lower values (< 1.6) and slight differences among the PA/

PANO groups. A potential relationship between VIP and PA/PANO detection could be due to a multiplicity of interferences that are discussed in the following section.

Fig. 3 Variable importance in projection (VIP) and predictive scores by partial least squares discriminant analysis (PLS-DA) and canonical discriminant analysis (CDA) models for the three quantitative classes of pyrrolizidine alkaloids (PAs) and their *N*-oxides (PANOs) in bee pollen, based on lab-stationary (Foss, upper panel) and portable (Polispec, lower panel) near-infrared (NIR) systems. VIP scores are presented as trends throughout the entire spectral range and the CDA selected predictive wavelengths as vertical bars according to the canonical structure correlation coefficient (CDA predictive scores). Quantitative ($\mu\text{g}/\text{kg}$) PA/PANO classes: < LOQ (0.4), low; 0.4–400, moderate; > 400, high



CDA based on NIR spectral data

The main purpose of this study was to apply a multivariate pattern recognition method to determine the functional relationship between spectral NIR data and the presence of PAs/PANOs in a set of bee pollen samples, simulating a rapid screening to enhance the safety of on-market operating conditions. Among the supervised discriminating methods, CDA has been already proposed as a statistical model able to classify a sub-population of samples within a specific genetic, geographical or chemical class (e.g., PA/PANO amount) according to the similarity of a huge set of chemometric variables such as the NIR spectra

[30]. Despite being less frequently applied, the CDA algorithm allows a reduction of data redundancy, thus the discriminating power is preserved in the first canonical discriminant function [44]. Even though CDA seems to improve the classification accuracy when spatial separation of the experimental groups is achieved by the use of a large number of closed-spectral signatures, the use of a large dataset with too many highly correlated variables could be inappropriate for selecting the more informative wavelengths avoiding the irrelevant ones [32, 45]. Indeed, a data arrangement is required when a dataset has too many irrelevant variables, a high multicollinearity among instrumental signals and a number of predictors larger than

the sample size [46]. Therefore—in the case of the Foss system—before the stepwise selection, the dataset was restricted to 207 averaged spectral variables so that each one represents a 16 nm wavelength range (from λ_{854} to λ_{2494}). The portable NIR system presents a short window for spectral acquisition and a relatively longer measurement interval (2 nm); hence, there was no need to restrict the original dataset composed of 390 spectral variables.

For the lab-stationary NIR system (Foss), the stepwise procedure selected 18 significant averaged wavelengths: λ_{1162} , λ_{1250} , λ_{1330} , λ_{1362} , λ_{1418} , λ_{1514} , λ_{1682} , λ_{1746} , λ_{1850} , λ_{1930} , λ_{1994} , λ_{2042} , λ_{2074} , λ_{2186} , λ_{2218} , λ_{2250} , λ_{2322} and λ_{2474} . These spectral variables were used to perform the CDA algorithm that defined two significant functions, CAN1 and CAN2 (Wilks's $\lambda = 0.19$, approximate F value = 2.85, $df1 = 30$, $df2 = 80$, $p < 0.001$), which explained 78.9% and 21.1% of the total variability, respectively. Regarding the portable NIR system, 22 wavelengths were sorted as the most informative by the stepwise procedure: λ_{1146} , λ_{1158} , λ_{1172} , λ_{1186} , λ_{1200} , λ_{1226} , λ_{1270} , λ_{1324} , λ_{1332} , λ_{1344} , λ_{1368} , λ_{1416} , λ_{1442} , λ_{1460} , λ_{1484} , λ_{1514} , λ_{1534} , λ_{1576} , λ_{1588} , λ_{1632} , λ_{1652} and λ_{1680} . The CDA algorithm defined two canonical functions (CAN1 and CAN2) that showed a high discriminative power (Wilks's $\lambda = 0.25$, approximate F value = 1.59, $df1 = 44$, $df2 = 72$, $p = 0.039$), which accounted for 71.6% and 28.4% of the total variability, respectively. As shown in Fig. 4, for both NIR systems the CDA model highlighted the possibility of separating the 0.95 confidence circles for population centroids, especially the low class from the others. This discriminative capacity was confirmed by the significant D^2 -Mahalanobis values, which were equal to 9.5 ($p < 0.001$) between low and moderate classes, and 16.1 ($p < 0.001$) between low and high classes for Foss, and 7.7 ($p = 0.023$) between low and moderate classes, and 9.9 ($p = 0.022$), between low and high classes for Polisppec.

Furthermore, a confusion matrix obtained by leave-one-out cross-validation confirmed that the CDA classification functions allowed the correct assignment of each sample to its actual PA/PANO class based on the restricted pool of the selected NIR features (Table 2). Overall, both NIR spectrometers showed an accurate prediction of the absence of PAs/PANOs because of the high values of predictive parameters for the low class, as summarised by the MCC values of 0.96 and 0.91 for Foss and Polisppec, respectively. Conversely, assessment of the high class by the NIR-based algorithm highlighted a decrease in discriminant performance that was more relevant for the portable apparatus (MCC of 0.73 versus 0.59), even though no sample was misclassified as low class (Table 2). Considering the hypothesis of rapid spectroscopy-based screening for the absence (low class) and presence of PAs/PANOs (fusion of moderate and high classes), both NIR systems showed a false negative misclassification rate equal to 0.02

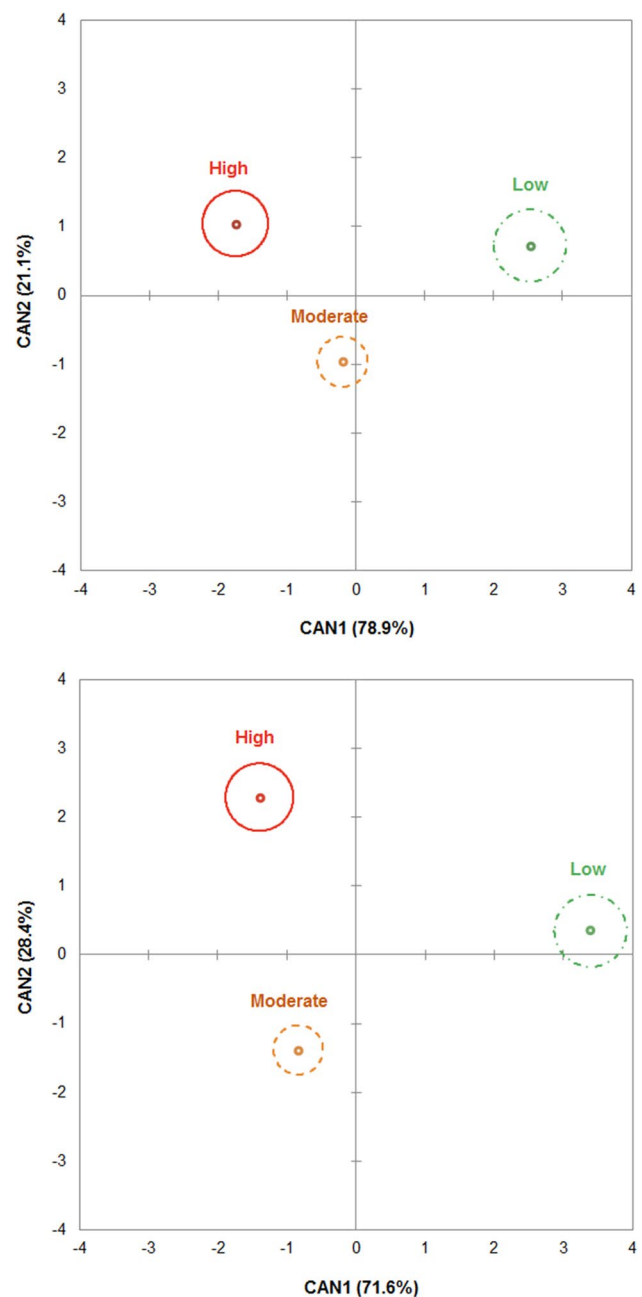


Fig. 4 Biplots of the 0.95 confidence circles around the centroids for the three quantitative classes of pyrrolizidine alkaloids (PAs) and their *N*-oxides (PANOs) in bee pollen, based on lab-stationary (Foss, upper panel) and portable (Polisppec, lower panel) near-infrared (NIR) systems. Quantitative ($\mu\text{g}/\text{kg}$) PA/PANO classes: <LOQ (0.4), low; 0.4–400, moderate; and > 400, high

(1 out of 46), which refers to a sample from the moderate class that was recognised as from the low class. That value is lower than the 0.05 threshold for false negatives usually applied in toxicological screening tests [47]. For Polisppec, there was also a false-positive misclassification rate of 0.07 (1 out of 14) related to wrong assignment of a

Table 2 Confusion matrix and descriptive statistics in cross-validation (leave-one-out criterion) for the three quantitative classes of pyrrolizidine alkaloids (PAs) and their *N*-oxides (PANOs) in ground bee pollen based on laboratory (Foss) and portable (Polispec) near-infrared (NIR) systems

	Foss			Predicted	Polispec		
	Actual				Actual		
Predicted	Low	Moderate	High	Predicted	Low	Moderate	High
Low	14	1	0	Low	13	1	0
Moderate	0	24	3	Moderate	1	22	5
High	0	4	14	High	0	6	12
Total	14	29	17	Total	14	29	17
Sensitivity	1.00	0.83	0.82		0.93	0.76	0.71
Specificity	0.98	0.90	0.91		0.98	0.81	0.86
Accuracy	0.98	0.87	0.88		0.97	0.78	0.82
Precision	0.93	0.89	0.78		0.93	0.79	0.67
MCC	0.96	0.75	0.73		0.91	0.61	0.59

Quantitative ($\mu\text{g}/\text{kg}$) PA/PANO classes: <LOQ (0.4), low; 0.4–400, moderate; and > 400, high; bold values represent the samples classified correctly

MCC Matthews correlation coefficient

sample from the low class to the moderate class, but this represents only an additional charge because it implies further confirmatory analysis by LC–MS/MS, which is the analytical technique recommended by food safety authorities.

The outcomes of this study indicate the potential capability of NIR spectroscopy to perform reliable screening of bee pollen samples contaminated with PAs/PANOs. Indeed, these natural toxins significantly affected the spectral data, indicating that the NIR technology can be applied for a rapid evaluation of the presence of contaminants [48]. However, as underlined by the decrease in the sensitivity and specificity values (Table 2), the attempt to distinguish a moderate from a high level of PAs/PANOs seems to be partially predictable, probably due to the chemical structure and stereochemistry of these molecules, which influence their toxicity and physical–optical properties [49].

The slightly lower capability of the tested portable NIR instrument is in agreement with the literature. This phenomenon is probably due to worse optical properties and the negative interference of the field operative conditions compared to the lab-stationary apparatus [26, 50], even though its flexibility and the possibility of application at/in-line represent major advantages.

The CDA algorithm (by means of the canonical standardised coefficient) highlighted a relatively similar explicative power of all the predictors because their loading values (predictive scores) ranged from 0.30 to 0.50 and these selected wavelengths involved the spectral region > 1150 nm (Fig. 3). Among them, within the 1140–1370 nm region, λ_{1162} , λ_{1250} , λ_{1330} and λ_{1362} (Foss) and λ_{1146} , λ_{1158} , λ_{1172} , λ_{1200} , λ_{1226} , λ_{1270} , λ_{1324} , λ_{1332} , λ_{1344} and λ_{1368} (Polispec) could be related to C–H stretching second overtones [51]. The absorption bands λ_{1418} (Foss) and λ_{1416} (Polispec) can be related to O–H stretching first overtones of R–OH [52] that are present in the

chemical structure of PAs/PANOs. The predictors λ_{1442} and λ_{1460} (Polispec) could be associated with the first overtones of cyclic amines [52], which compose the basic structure of all PAs/PANOs. In relation to these latter selected wavelengths, the 1400 nm has been already suggested as a shared region between tertiary-amines and *N*-oxides, where these molecules seemed to interact with electromagnetic radiation, resulting in vibrational spectroscopic signals [25]. Although the *N*-oxide spectrum is related to many wavelengths in the visible and infrared regions, the interpretation of the spectroscopic dynamic behaviour of the structure of PANOs is still lacking [53]. Another region that can also be affected by cyclic amines is within the 1900–2100 nm region [25], represented by λ_{1930} , λ_{1994} , λ_{2042} and λ_{2074} (Foss). The CDA feature stepwise procedure also sorted some informative wavelengths between 1500 and 1590 nm, including λ_{1514} (Foss) and λ_{1514} , λ_{1534} , λ_{1576} and λ_{1588} (Polispec). These wavelengths may be influenced by stretch overtones of O–H and combination bands of N–H with C=O, and C–N stretching of amine/amide structures [25]. The absorption peak at λ_{1850} (Foss) may be related to the second overtone of C=O stretching of carboxyl groups [52], which are also found in the PA/PANO chemical structure. Some of these alkaloids can also contain epoxide–amine structures that may influence the λ_{1632} , λ_{1652} (Polispec) and λ_{2218} (Foss) regions [25]. In the case of the Foss spectrometer, the selected wavelengths of λ_{2186} , λ_{2218} , λ_{2250} , λ_{2322} and λ_{2474} can be considered informative NIR variables because they correspond to combination bands of N–H from amines/amides and O–H from alcohols, and C–H and C–C stretching from –CH, –CH₂ and –CH₃ [43, 54].

Conclusions

The outcomes of this work highlighted that over 75% of the 60 bee pollen samples analysed were contaminated with PAs/PANOs, even though less than 30% might have a concentration higher than the threshold of 400 µg/kg used for the NIR analyses. However, a relevant variability was observed in the distribution of the 17 PAs/PANOs monitored, as confirmed by the relevant values of standard deviation within both moderate and high classes, which represent a classification method below or above the threshold of 400 µg/kg.

The presence of the PAs/PANOs in bee pollen significantly affected the NIR spectra, highlighted a rising level of absorbance as their concentration increased. This outcome suggests that their chemical structure interferes with the light scattering throughout many band regions. The application of CDA resulted in a modelling statistical approach that demonstrates the predictive capacity of NIR systems to distinguish among the three quantitative PA/PANO classes, especially for detection of those samples belonging to the low class, which corresponds to safe samples.

In summary, both NIR systems have the potential to be applied for rapid and reliable identification of contaminated bee pollens in large-scale screening in the food supply chain by also using an at-line operating system, however, the laboratory might be considered the more feasible NIR tool to achieve this purpose. PA/PANO detection could be strengthened by applying a chemometric approach based on a further informative dataset shared among the research community and food safety agencies.

Acknowledgements This work was funded by the University of Padova (CPDA 158894/15 project) and FONDAZIONE CARIVERONA (call 2016-SAFIL project).

Funding Open access funding provided by Università degli Studi di Padova within the CRUI-CARE Agreement.

Compliance with ethical standards

Conflict of interest The authors declare that they have no known competing financial interests or personal relationships that could have appeared to influence the work reported in this paper.

Compliance with ethics requirements This article does not contain any studies with human participants or animal performed by any of the authors.

Open Access This article is licensed under a Creative Commons Attribution 4.0 International License, which permits use, sharing, adaptation, distribution and reproduction in any medium or format, as long as you give appropriate credit to the original author(s) and the source, provide a link to the Creative Commons licence, and indicate if changes were made. The images or other third party material in this article are included in the article's Creative Commons licence, unless indicated otherwise in a credit line to the material. If material is not included in

the article's Creative Commons licence and your intended use is not permitted by statutory regulation or exceeds the permitted use, you will need to obtain permission directly from the copyright holder. To view a copy of this licence, visit <http://creativecommons.org/licenses/by/4.0/>.

References

1. Denisow B, Denisow-Pietrzyk M (2016) Biological and therapeutic properties of bee pollen: a review. *J Sci Food Agric* 96:4303–4309
2. Boppré M, Colegate SM, Edgar JA, Fischer OW (2008) Hepato-toxic pyrrolizidine alkaloids in pollen and drying-related implications for commercial processing of bee pollen. *J Agric Food Chem* 56:5662–5672. <https://doi.org/10.1021/jf800568u>
3. EFSA (2011) Scientific opinion on pyrrolizidine alkaloids in food and feed: EFSA panel on contaminants in the food chain (CONTAM). *EFSA J* 9:1–134. <https://doi.org/10.2903/j.efsa.2011.2406>
4. Fu PP, Xia Q, Lin G, Chou MW (2004) Pyrrolizidine alkaloids—genotoxicity, metabolism enzymes, metabolic activation, and mechanisms. *Drug Metab Rev* 36:1–55. <https://doi.org/10.1081/DMR-120028426>
5. Moreira R, Pereira DM, Valentão P, Andrade PB (2018) Pyrrolizidine alkaloids: chemistry, pharmacology, toxicology and food safety. *Int J Mol Sci* 19:1–22. <https://doi.org/10.3390/ijms19061668>
6. Merz KH, Schrenk D (2016) Interim relative potency factors for the toxicological risk assessment of pyrrolizidine alkaloids in food and herbal medicines. *Toxicol Lett* 263:44–57. <https://doi.org/10.1016/j.toxlet.2016.05.002>
7. Gottschalk C, Huckauf A, Dübecke A et al (2018) Uncertainties in the determination of pyrrolizidine alkaloid levels in naturally contaminated honeys and comparison of results obtained by different analytical approaches. *Food Addit Contam Part A Chem Anal Control Expo Risk Assess* 35:1366–1383. <https://doi.org/10.1080/19440049.2018.1468929>
8. EFSA (2017) Risks for human health related to the presence of pyrrolizidine alkaloids in honey, tea, herbal infusions and food supplements. *EFSA J* 15(7):1–34. <https://doi.org/10.2903/j.efsa.2017.4908>
9. BFR (Federal Institute for Risk Assessment)(2011) Chemical analysis and toxicity of pyrrolizidine alkaloids and assessment of the health risks posed by their occurrence in honey. BFR opinion No. 038/2011. Available online: <https://www.bfr.bund.de/cm/349/chemical-analysis-and-toxicity-of-pyrrolizidine-alkaloids-and-assessment-of-the-health-risks-posed-by-their-occurrence-in-honey.pdf>. Accessed 28 Apr 2020
10. Committee on toxicity of chemicals in food consumer products and the environment (2008) COT statement on pyrrolizidine alkaloids in food. cot.food.gov.uk/pdfs/cotstatementpa200806.pdf
11. Hurtado MC, Conchello Moreno MP, Daschner Á et al (2018) Informe del Comité Científico de la Agencia Española de Seguridad Alimentaria y Nutrición (AESAN) sobre el riesgo asociado a la presencia de alcaloides de la pirrolizidina en polen destinado al consumo humano. *Rev del Com Científico la AESAN* 28:127–140
12. EFSA (2016) Dietary exposure assessment to pyrrolizidine alkaloids in the European population. *EFSA J*. <https://doi.org/10.2903/j.efsa.2016.4572>
13. Agencia Española de Consumo SA y N (AECOSAN) (2019) Alcaloides De Pirrolizidina. https://www.aecosan.msssi.gob.es/AECOSAN/docs/documentos/seguridad_alimentaria/gestion_riesgos/PAs_ficha.pdf. Accessed 19 May 2020

14. AFEPADI (2019) Alcaloides de pirrolizidina. ¿Próxima limitación? In: Asoc. las Empres. Dietéticos y Complement. Aliment. <https://www.afepadi.org/index.php/component/k2/item/442-alcaloides-de-pirrolizidina-proxima-limitacion>. Accessed 10 Mar 2020
15. UK FSA (2019) June 2019 Stakeholder Update on Rapidly Developing Policy on food contaminants environmental and industrial contaminants. <https://www.food.gov.uk/news-alerts/consultations/june-2019-stakeholder-update-on-rapidly-developing-policy-on-food-contaminants>. Accessed 20 May 2020
16. BfR (Federal Institute for Risk Assessment) (2018) Updated risk evaluation of levels of 1, 2-unsaturated pyrrolizidine alkaloids (PA) in foods. BfR Opin 20:1–2. <https://doi.org/10.17590/20180730-085425-0>
17. Mulder PJJ, López P, Castelari M et al (2018) Occurrence of pyrrolizidine alkaloids in animal- and plant-derived food: results of a survey across Europe. Food Addit Contam Part A Chem Anal Control Expo Risk Assess 35:118–133. <https://doi.org/10.1080/19440049.2017.1382726>
18. Picron J, Herman M, Van Hoeck E, Gosciny S (2019) Monitoring of pyrrolizidine alkaloids in beehive products and derivatives on the Belgian market. Environ Sci Pollut Res. <https://doi.org/10.1007/s11356-019-04499-2>
19. Sixto A, Niell S, Heinzen H (2019) Straightforward determination of pyrrolizidine alkaloids in honey through simplified methanol extraction (QuPPE) and LC–MS/MS modes. ACS Omega 4:22632–22637. <https://doi.org/10.1021/acsomega.9b03538>
20. Alander JT, Bochko V, Martinkauppi B et al (2013) A review of optical nondestructive visual and near-infrared methods for food quality and safety. Int J Spectrosc. <https://doi.org/10.1155/2013/341402>
21. Hernández-Hierro JM, García-Villanova RJ, González-Martín I (2008) Potential of near infrared spectroscopy for the analysis of mycotoxins applied to naturally contaminated red paprika found in the Spanish market. Anal Chim Acta 622:189–194. <https://doi.org/10.1016/j.aca.2008.05.049>
22. De Girolamo A, von Holst C, Cortese M et al (2019) Rapid screening of ochratoxin A in wheat by infrared spectroscopy. Food Chem 282:95–100. <https://doi.org/10.1016/j.foodchem.2019.01.008>
23. Mishra P, Diezma B, Barreiro P (2015) NIR hyperspectral imaging for detection of nut contamination. New Food 18:30–33
24. Radman M, Jurina T, Benković M et al (2018) Application of NIR spectroscopy in gluten detection as a cross-contaminant in food. Croat J Food Technol Biotechnol Nutr 13:120–127. <https://doi.org/10.31895/hcptbn.13.3-4.4>
25. Carvalho S, Macel M, Schlerf M et al (2013) Changes in plant defense chemistry (pyrrolizidine alkaloids) revealed through high-resolution spectroscopy. ISPRS J Photogramm Remote Sens 80:51–60. <https://doi.org/10.1016/j.isprsjprs.2013.03.004>
26. Teixeira Dos Santos CA, Lopo M, Páscoa RNMJ, Lopes JA (2013) A review on the applications of portable near-infrared spectrometers in the agro-food industry. Appl Spectrosc 67:1215–1233. <https://doi.org/10.1366/13-07228>
27. Crocombe RA (2018) Portable spectroscopy. Appl Spectrosc 72:1701–1751. <https://doi.org/10.1177/0003702818809719>
28. Campos MGR, Bogdanov S, de Almeida-Muradian LB et al (2008) Pollen composition and standardisation of analytical methods. J Apic Res 47:154–161. <https://doi.org/10.1080/00218839.2008.11101443>
29. Anjos O, Santos AJA, Dias T, Estevinho LM (2017) Application of FTIR-ATR spectroscopy on the bee pollen characterization. J Apic Res 56:210–218. <https://doi.org/10.1080/00218839.2017.1289657>
30. De Jesus Inacio L, Merlanti R, Lucatello L et al (2020) Pyrrolizidine alkaloids in bee pollen identified by LC-MS/MS analysis and colour parameters using multivariate class modeling. Heliyon 6:e03593. <https://doi.org/10.1016/j.heliyon.2020.e03593>
31. Lucatello L, Merlanti R, Rossi A et al (2016) Evaluation of some pyrrolizidine alkaloids in honey samples from the Veneto Region (Italy) by LC–MS/MS. Food Anal Methods 9:1825–1836. <https://doi.org/10.1007/s12161-015-0364-7>
32. Segato S, Merlanti R, Bisutti V et al (2019) Multivariate and machine learning models to assess the heat effects on honey physicochemical, colour and NIR data. Eur Food Res Technol 245:2269–2278. <https://doi.org/10.1007/s00217-019-03332-x>
33. Bisutti V, Merlanti R, Serva L et al (2019) Multivariate and machine learning approaches for honey botanical origin authentication using near infrared spectroscopy. J Near Infrared Spectrosc 27:65–74. <https://doi.org/10.1177/096703518824765>
34. Martinello M, Cristofoli C, Gallina A, Mutinelli F (2014) Easy and rapid method for the quantitative determination of pyrrolizidine alkaloids in honey by ultra performance liquid chromatography-mass spectrometry: an evaluation in commercial honey. Food Control 37:146–152. <https://doi.org/10.1016/j.foodcont.2013.09.037>
35. Kast C, Kilchenmann V, Reinhard H et al (2019) Pyrrolizidine alkaloids: the botanical origin of pollen collected during the flowering period of *Echium vulgare* and the stability of pyrrolizidine alkaloids in bee bread. Molecules. <https://doi.org/10.3390/molecules24122214>
36. Schramm S, Köhler N, Rozhon W (2019) Pyrrolizidine alkaloids: biosynthesis, biological activities and occurrence in crop plants. Molecules 24:498. <https://doi.org/10.3390/molecules24030498>
37. Stegemann T, Kruse LH, Brütt M, Ober D (2019) Specific distribution of pyrrolizidine alkaloids in floral parts of comfrey (*Symphytum officinale*) and its implications for flower ecology. J Chem Ecol 45:128–135. <https://doi.org/10.1007/s10886-018-0990-9>
38. Flade J, Beschow H, Wensch-Dorendorf M et al (2019) Occurrence of nine pyrrolizidine alkaloids in *Senecio vulgaris* L. Depending on developmental stage and season. Plants 8:1–13. <https://doi.org/10.3390/plants8030054>
39. Stegelmeier B, Edgar J, Colegate S et al (1999) Pyrrolizidine alkaloid plants, metabolism and toxicity. J Nat Toxins 8:95–116. <https://doi.org/10.1023/B:PHAM.0000016235.32639.23>
40. Kast C, Kilchenmann V, Reinhard H et al (2018) Chemical fingerprinting identifies *Echium vulgare*, *Eupatorium cannabinum* and *Senecio* spp. as plant species mainly responsible for pyrrolizidine alkaloids in bee-collected pollen. Food Addit Contam Part A Chem Anal Control Expo Risk Assess 35:316–327. <https://doi.org/10.1080/19440049.2017.1378443>
41. Pasikatan MC, Steele JL, Spillman CK, Haque E (2001) Near infrared reflectance spectroscopy for online particle size analysis of powders and ground materials. J Near Infrared Spectrosc 9:153–164. <https://doi.org/10.1255/jnirs.303>
42. González-Martín I, Hernández-Hierro JM, Barros-Ferreiro N et al (2007) Use of NIRS technology with a remote reflectance fibre-optic probe for predicting major components in bee pollen. Talanta 72:998–1003. <https://doi.org/10.1016/j.talanta.2006.12.039>
43. Costa MCA, Morgano MA, Ferreira MMC, Milani RF (2017) Analysis of bee pollen constituents from different Brazilian regions: quantification by NIR spectroscopy and PLS regression. LWT Food Sci Technol 80:76–83. <https://doi.org/10.1016/j.lwt.2017.02.003>
44. Zhao G, Maclean AL (2000) A comparison of canonical discriminant analysis and principal component analysis for spectral transformation. Photogramm Eng Remote Sensing 66:841–847
45. Leardi R (2000) Application of genetic algorithm-PLS for feature selection in spectral data sets. J Chemom 14:643–655. [https://doi.org/10.1002/1522-2675\(200007\)14:6<643::AID-JCHEMOM643>3.0.CO;2-3](https://doi.org/10.1002/1522-2675(200007)14:6<643::AID-JCHEMOM643>3.0.CO;2-3)

- [://doi.org/10.1002/1099-128X\(200009/12\)14:5/6<643:AID-CEM621>3.0.CO;2-E](https://doi.org/10.1002/1099-128X(200009/12)14:5/6<643:AID-CEM621>3.0.CO;2-E)
46. Akarachantachote N, Chadcham S, Saithanu K (2014) Cut-off threshold of variable importance in projection for variable selection. *Int J Pure Appl Math* 94:307–322. <https://doi.org/10.12732/ijpam.v94i3.2>
 47. Opladowska M, Elliott CT, Huet AC et al (2014) Development and validation of a rapid multiplex ELISA for pyrrolizidine alkaloids and their *N*-oxides in honey and feed rapid detection in food and feed. *Anal Bioanal Chem* 406:757–770. <https://doi.org/10.1007/s00216-013-7488-7>
 48. Shen F, Wu Q, Shao X, Zhang Q (2018) Non-destructive and rapid evaluation of aflatoxins in brown rice by using near-infrared and mid-infrared spectroscopic techniques. *J Food Sci Technol* 55:1175–1184. <https://doi.org/10.1007/s13197-018-3033-1>
 49. Villanueva-Cañongo C, Pérez-Hernández N, Hernández-Carlos B et al (2014) Complete ¹H NMR assignments of pyrrolizidine alkaloids and a new eudesmanoid from *Senecio polypodioides*. *Magn Reson Chem* 52:251–257. <https://doi.org/10.1002/mrc.4054>
 50. Marchesini G, Serva L, Garbin E et al (2017) Near-infrared calibration transfer for undried whole maize plant between laboratory and on-site spectrometers. *Ital J Anim Sci*. <https://doi.org/10.1080/1828051X.2017.1345660>
 51. He J, Chen L, Chu B, Zhang C (2018) Determination of total polysaccharides and total flavonoids in *Chrysanthemum morifolium* using near-infrared hyperspectral imaging and multivariate analysis. *Molecules* 23:1–13. <https://doi.org/10.3390/molecules23092395>
 52. Weyer LG (1985) Near-infrared spectroscopy of organic substances. *Appl Spectrosc Rev* 21:1–43. <https://doi.org/10.1080/05704928508060427>
 53. Oliveira RP, Demuner AJ, Alvarenga ES et al (2017) Experimental and theoretical studies on the characterization of monocrotaline by infrared and Raman spectroscopies. *J Mol Struct* 1135:228–233. <https://doi.org/10.1016/j.molstruc.2017.01.050>
 54. Márquez C, López MI, Ruisánchez I, Callao MP (2016) FT-Raman and NIR spectroscopy data fusion strategy for multivariate qualitative analysis of food fraud. *Talanta* 161:80–86. <https://doi.org/10.1016/j.talanta.2016.08.003>

Publisher's Note Springer Nature remains neutral with regard to jurisdictional claims in published maps and institutional affiliations.